2024 IEEE/ASME International Conference on Advanced Intelligent Mechatronics (AIM)
July 15-19, 2024. Boston, MA, USA

2024 IEEE/ASME International Conference on Advanced Intelligent Mechatronics (AIM) | 979-8-3503-5536-9/24/$31.00 ©2024 IEEE | DOI: 10.1109/AIM55361.2024.10636948

Algorithm for Locomotion Mode Selection, Energy Estimation and Path Planning for a Multi-terrain Screw-Propelled Vehicle for Arctic Exploration

Sumedh Beknalkar[1] Matthew Bryant[2] and Andre Mazzoleni[3]

***Abstract*— The Multi-terrain Amphibious ARCtic explOrer or MAARCO is a screw-propelled vehicle designed to move seamlessly across the heterogeneous and diverse Arctic landscape. Its propulsion system consists of one or multiple pairs of helical drives (or Archimedes' screws) that offer two modes of locomotion for straight-line motion while moving on land - *Screw* and *Crab-crawl*. In screw mode, the rover moves in a forward or backward direction by rotating the drives in opposite directions at the same speed. While in crab-crawl mode, the rover moves sideways by rotating the drives in the same direction at the same speed. This paper presents an algorithm for selecting between two modes of locomotion for straight-line motion as a function of the terrain or substrate that the rover is traversing. The algorithm is further applied for performing energy estimation and path planning. Results show that the rover chooses crab-crawl mode if the substrate fails under the stresses exerted by the rover and vice versa. The path planning section of the algorithm shows that maximizing the distance traveled in crab-crawl mode while simultaneously minimizing the distance traveled in screw mode derives the path with the least amount of required energy.**

I. INTRODUCTION

Global warming has led to the melting of expansive tracts of ice in the polar regions resulting in rising sea levels and ever-changing climate patterns. The need to study the effect of global warming in the polar regions has led to the development of autonomous robots that can operate in areas that are inaccessible and dangerous to humans. However, the heterogeneous and rugged terrain conditions in the Arctic pose significant challenges to the autonomous locomotion capabilities that are not met by current rover technology [1]–[3]. A robot deployed in the Arctic must be highly adaptable to the diverse terrain conditions and must be able to traverse on land, on water, and underwater.

The proposed **M**ulti-terrain **A**mphibious **ARC**tic expl**O**rer or **MAARCO** rover is a multi-terrain and amphibious robot capable of moving seamlessly across the diverse terrains in the Arctic [4]–[9]. The rover uses a mechanically simple, potentially low-cost propulsion system called helical drives or Archimedes' screws, which are screw-like rotating central cylinders with helix-shaped blades. On snow, mud, and snow, the helical blades push back on the surface medium to produce propulsion. In water, the central cylinders offer can be flooded or emptied to make the rover float on water (using positive buoyancy) or operate underwater (using neutral or negative buoyant while the rotating blades produce thrust. The multi-terrain and amphibious locomotion capabilities will enable MAARCO to traverse the heterogeneous landscape in the Arctic.

While moving on land, the simple yet functional propulsion system offers two modes of locomotion:

Screw mode: In screw mode, the rover moves forward or backward by rotating the drives in opposite directions.

Crab-crawl mode: In crab-crawl mode, the rover moves sideways to the left (port) or right (starboard) by rotating the drives in the same direction.

Whether the rover can move in *screw* or *crab-crawl* mode depends on the relative magnitudes and directions of the propulsive forces acting on the blades and the traction forces acting on the cylinders. The relative direction of the propulsive and traction forces depends on the rotational directions of the two helical drives. However, their magnitudes depend on the bulk properties of the surrounding substrates. Thus, for a helical drives-based rover with a fixed design, the rover's mode of locomotion depends on the substrate the rover is traversing and hence, there is a need for a control strategy that will determine the optimal mode of locomotion (screw vs crab-crawl) depending on the surrounding substrate.

In recent decades, there has been a resurgence of helical drives-based vehicles for planetary and extraplanetary exploration [10], [11]. The advent of modern computational and experimental tools has resulted in a better understanding of terrestrial locomotion dynamics and control of helical drives on soft and granular media [12]–[14]. However, there exists a gap in the literature related to the selection of between screw and crab-crawl modes as a function of the surrounding substrate. The work in this paper attempts to address the control challenge posed by a screw-propelled vehicle by developing an algorithm for mode selection. Additionally, the algorithms is also used for energy estimation and path planning.

The rest of the paper is organized as follows: Section II discusses the locomotion in screw mode while Section III discusses the locomotion in crab-crawl mode. Section IV

*The authors gratefully acknowledge funding for this research provided by the National Science Foundation under award "MAARCO – Multi-terrain Amphibious ARCtic ExplOrer", award no. CMMI-2116216, which is managed by Dr. Alex Leonessa

[1]Sumedh Beknalkar is a PhD student in the Department of Mechanical and Aerospace Engineering at North Carolina State University Raleigh, NC 27695 sbeknal@ncsu.edu

[2]Matthew Bryant is an Associate Professor in the Department of Mechanical and Aerospace Engineering at North Carolina State University Raleigh, NC 27695 mbryant@ncsu.edu

[3]Andre Mazzoleni is a Professor in the Department of Mechanical and Aerospace Engineering at North Carolina State University Raleigh, NC 27695 apmazzoleni@ncsu.edu

discusses the steps involved in selecting a mode between screw and crab-crawl modes followed by the energy estimation and path planning. Section V discusses the results of the application of the algorithm for a hypothetical landscape.

II. SCREW MODE

Fig. 1 shows a schematic of the proposed MAARCO rover. The rover body has two helical drives, a central console, and a chassis with four chassis legs. The torques acting on the helical drives control the angular accelerations and thereby the angular speed of the helical drives. In this paper, the rover is assumed to be moving on a perfectly flat surface and hence, a two-dimensional model of the locomotion dynamics of MAARCO has been considered.

In screw mode, the rover moves in a forward or backward direction as shown in Fig 2. Straight line motion in screw mode is achieved when the left and right helical drives rotate at the same angular speed but in opposite directions. The dynamic model for locomotion in screw mode was developed in the authors' previous work in [5] but is summarized below for the benefit of the reader. The forces acting on the helical drive are (i) the propulsive forces on the helical blades (N_L and N_R), (ii) the friction forces on the central cylinder ($F_{c,L}$ and $F_{c,R}$), (iii) the friction force on the blades ($F_{b,L}$ and $F_{b,R}$). All forces are assumed to be acting through a single point located at a distance r (which is the effective radius) from the center of mass of the drives. These forces and the directions in which they act are shown in 2. The propulsive forces act normal to the surface of the helical blades while the friction forces act in a direction opposite to the angle ϕ where $tan(\phi)$ is the ratio of the linear (v) and rotational ($r \cdot \omega$) speeds of the helical drive, i.e., $tan(\phi) = \frac{v}{r\omega}$. The angle ψ is the pitch angle of the helical drive. It is related to the pitch length (P) and radius (r) of helical drives as follows: $tan(\psi) = \frac{P}{2\pi r}$.

The governing equations of steady-state motion in screw mode while moving in a straight line for the left helical drive are [5]:

$$N_L\, cos(\psi) - F_{c,L}\, sin(\phi) - F_{b,L}\, sin(\phi) = 0 \qquad (1)$$

$$T_{screw,L} - r(N_L\, sin(\psi) + F_{c,L}\, cos(\phi) + F_b\, cos(\phi)) = 0 \qquad (2)$$

Here, (1) represents that the force balance in the x-direction (the direction of motion), while (2) represents the torque balance on each helical drive. In (2), $T_{screw,L}$ is the required torque per motor that is commanded by the rover. Equation (1) is used to calculate N_L and (2) is used to calculate $T_{screw,L}$. The equations for the right drive are identical in form to those of the left drive.

A. Locomotion characteristics and Substrate Failure Check

As shown in [5], if the surrounding substrate does not fail under the shear stresses exerted by the helical drives, then the linear displacement of the center of mass of the helical drive (x_c) is pitch length (P) times the number of rotations of the helical drives, (n), i.e., $x_c = P \cdot n$. The

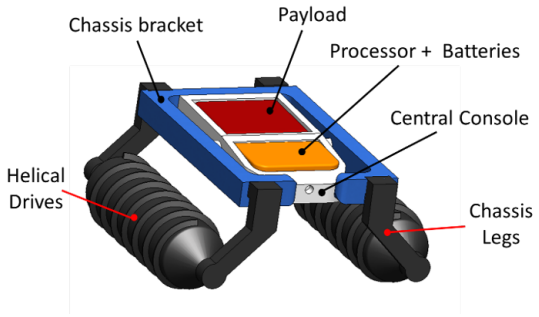

Fig. 1. Schematic of the MAARCO rover along with its components

motion of each helical drive resembles that of a "bolt through a threaded hole". $x_c = P \cdot n$ motion represents the best-case scenario for motion in screw mode. However, if the substrate fails under the stresses exerted by the helical drive, then $x_c < P \cdot n$ [5]. When the substrate fails and is in a state of equilibrium, it acts like a semi-solid or fluid and no longer acts like a rigid threaded hole. This results in a drastic decrease in propulsive force (N) as the substrate can no longer 'push against' the helical blades and moves like a fluid. Additionally, in $x_c < P \cdot n$ motion, the required motor torque (T_{screw}) increases since a portion of the torque is now utilized to move the fluid-like surrounding substrate while the rest is used to maintain helical drive motion.

Using the forces in Equation 1 and the dimensions of the annulus-shaped substrate element located between two helical blades, the maximum shear stress (τ_{max}) exerted by the helical drive on the substrate element is calculated. If the maximum shear stress is greater than the shear strength of the substrate (τ_{sub}), i.e., $\tau_{max} \geq \tau_{sub}$, then the substrate fails, $x_c < P \cdot n$ and the magnitude of N drops significantly. However, if $\tau_{max} < \tau_{sub}$, then and $x_c = P \cdot n$.

The shear strength of the substrate is calculated using the Mohr-Coulomb criterion:

$$\tau_{sub} = c + \sigma_{max,shear}\, tan(\phi_{fric}) \qquad (3)$$

where, c and ϕ_{fric} are the apparent cohesion and internal friction angle of the substrate, respectively. $\sigma_{max,shear}$ is the normal stress acting on the surface of maximum shear stress and is calculated using the principal stresses.

III. CRAB-CRAWL MODE

In crab-crawl mode, the rover moves laterally to its left or right as shown in Fig. 3. To achieve motion in crab-crawl mode, the left and right drives are rotated in the same direction and at the same angular speed. The drives act like rigid wheels or cylinders where the axes of rotational and translational motions are mutually perpendicular. The forces acting on the helical drives are shown in Fig. 3.

The traction forces (F_c) acting on the cylinders of the left and right helical drives point in the same direction resulting in motion in that direction. On the other hand, the propulsive force (N) acting on the left and right helical drive blades can cause a torque about the yaw axis causing the rover to turn

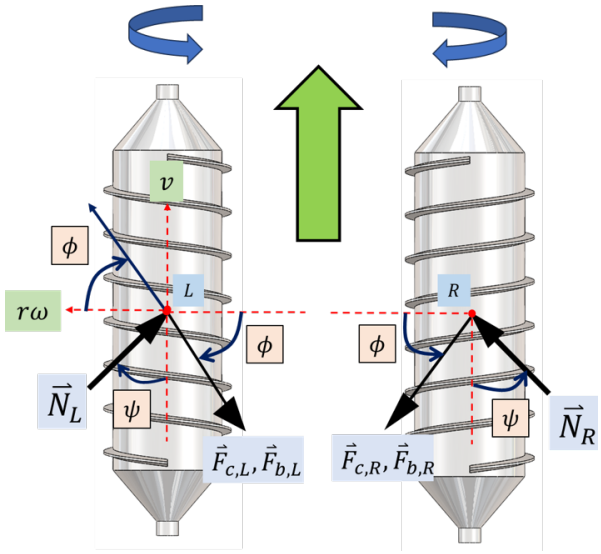

Fig. 2. Screw mode locomotion along with the forces acting on the helical drives. The friction forces oppose the net motion of the helical drive which is a combination of the on rotational motion ($r\omega$) and linear motion (v) of the helical drive

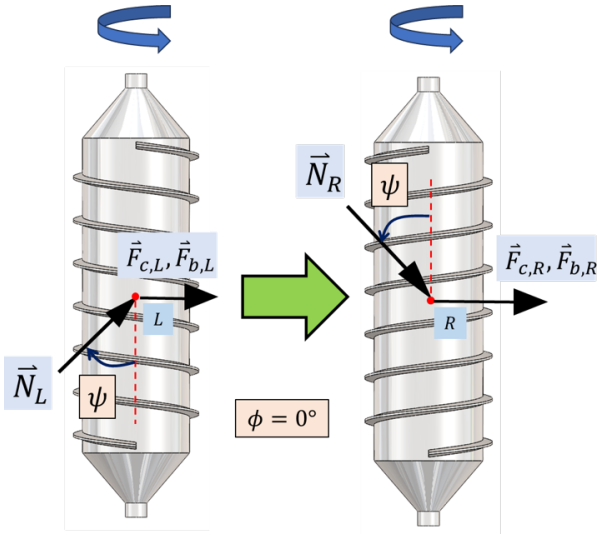

Fig. 3. Crab-crawl mode locomotion along with the forces acting on the helical drives. In this case, friction forces act as traction forces. Additionally, the angle between rotation and linear speeds is zero, hence $\phi = 0°$

left or right. However, in crab-crawl mode, the propulsive force acting on the blades is insignificantly small resulting in negligible yaw of the vehicle. In such a scenario, the helical drive acts like a rigid wheel or cylinder with a radius equal to the cylinder (r_c). Hence, the steady-state motion of a helical drive can be modeled based on the equilibrium equations of a wheel, described in [15] as follows:

$$F_z = r_c\, l_{HD}\Big(\int_{\theta_2}^{\theta_1} \sigma(\theta)cos\theta d\theta + \int_{\theta_2}^{\theta_1} \tau(\theta)sin(\theta)d\theta\Big) \quad (4)$$

$$F_x = r_c\, l_{HD}\Big(\int_{\theta_2}^{\theta_1} \tau(\theta)cos(\theta)d\theta - \int_{\theta_2}^{\theta_1} \sigma(\theta)sin\theta d\theta\Big) \quad (5)$$

$$T_{cc} = r_c^2\, l_{HD} \int_{\theta_2}^{\theta_1} \tau(\theta)d\theta \quad (6)$$

These equations assume that the wheel moves at a constant speed and zero acceleration, i.e., steady state, and that the stresses do not change along the width of the wheel (or in this case, the length of the helical drive (l_{HD})). The shape of the contact area is a cylindrical envelope with dimensions that depend on the wheel radius (r_c) and width (l_{HD}). $\sigma(\theta)$ and $\tau(\theta)$ are the normal (or radial) and tangential stresses exerted by the surrounding substrate on the wheel (or in this case, the helical drive). The normal and tangential stresses are a function of the angle θ which varies from the exit angle (θ_2) to the entry angle (θ_1), as shown in Fig. 4. F_z and F_x are the vertical and horizontal loads on the wheel. The first and second terms on the right-hand side of Equation 5 represent the thrust and motion resistance (or rolling resistance), respectively. Unless the rover is acted upon by a drawbar pull, the thrust and rolling resistance are equal while the wheel is in steady-state motion. Hence, in this case: $F_x = 0$. In (6), T_{cc} is the required torque per motor commanded by the rover in crab-crawl mode.

A. Sinkage and Slip of Wheel

The normal and tangential stresses acting on the wheel or helical drive, are functions of sinkage (z) and slip (i). The normal stress is related to the sinkage as follows [15]:

$$\sigma(\theta) = (k_\phi + \frac{k_c}{b})\, z^n \quad (7)$$

Here, k_ϕ, k_c, and n are pressure-sinkage parameters that are functions of the substrate type. b is the smaller dimension of the contact patch of the wheel with the substrate which is the diameter of the wheel, i.e., $b = 2\,r_c$. As can be seen in Fig. 4, sinkage z is a function of entry θ_1 and exit θ_2 angles.

The shear stress exerted by the substrate on the wheel depends on the shear deformation (or displacement) and the relationship between them is described as follows [15]:

$$\tau(\theta) = (c + \sigma\,(\theta) \cdot\, tan(\phi_{fric})\,(1 - e^{\frac{-j(\theta)}{K}}) \quad (8)$$

Here, $j(\theta)$ and K are the shear deformation and shear deformation modulus of the substrate. The shear deformation $j(\theta)$ depends on the slip velocity v_j of the wheel relative to the substrate, and is calculated using the following equations [15]:

$$v_j = r\,\omega[1 - (1 - i)\,cos(\theta)]$$
$$j = \int_0^t v_j\, dt = \int_{\theta_2}^{\theta_1} r\,[1 - (1 - i)\,cos(\theta)]\, d(\theta) \quad (9)$$

where, ω is the angular speed of the wheel. Thus, using $F_x = 0$ and the expressions for $\sigma(\theta)$ (from (7)), and $\tau(\theta)$ (from (8)) in (4) and (5), the sinkage (z) and slip (i) values are calculated. Then, substituting the values of using the expression for $\tau(\theta)$, the required motor torque (T_{cc}) is estimated through (6).

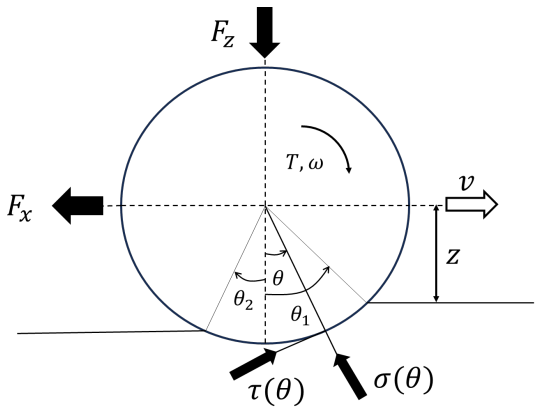

Fig. 4. Forces, torque, and stresses acting on a driven wheel (or helical drive in crab-crawl mode)

B. Locomotion characteristics and Slip

The motion of MAARCO while moving in a straight line using crab-crawl mode is a function of the circumference ($2\pi r_c$) of the cylinder and the wheel slip. The wheel slip is defined as $i = 1 - (v_c/\omega r_c)$. Using this expression, the linear motion of a wheel (or in this case a helical drive) is $x_c = (1-i)\theta r_c$, where θ is the angular displacement of the wheel. This means that the wheel or helical drive can move a linear distance anywhere from 0 to $2\pi r_c$ every rotation when slip varies from 0 to 1.

IV. ALGORITHM FOR MODE SELECTION, ENERGY ESTIMATION AND PATH PLANNING

The following assumptions were made in the development of the algorithm:

- The terrain parameters are known *a priori* and are fixed during the simulations.
- The surface of the terrain is flat and even

Additionally, the algorithm performs energy estimation and path planning based on steady-state, straight-line motion in both modes. It is assumed that the energy spent to transition from one mode to another is negligible and all paths considered by the algorithm are straight line paths. The energy estimation performed based on the above mentioned assumptions and simplifications is an early estimate of the energy required to execute a mission. A higher fidelity algorithm for mode selection, energy estimation, and path planning will be developed in future works.

A. Mode Selection

For a fixed rover design, the process of mode selection depends on the bulk factors of the substrate, the sinkage of helical drives as well as the forces acting on the helical drives.

1) Geometry of helical drives: The design of helical drives used in MAARCO and similar screw-propelled vehicles is such that the radius of the cylinder (r_c) is larger than the pitch length (P) of the helical blades. The large ballast radius requirement arises from the need to be positively buoyant while moving on water. Similarly, for a helical drive with a fixed length (l_{HD}), a small pitch length results in a small pitch angle and a helical drive with a small pitch length requires lower motor torque, $\tau_{motor,screw}$ (see (2) and [5]). This means that, because $r_c > P$, and more specifically $2\pi r_c > P$, the rover moves a greater distance per rotation in crab-crawl mode than in screw mode, and hence should be the preferred mode of locomotion. However, there exist two situations where crab-crawl mode cannot be used:

- When the yawing torque has a non-negligible magnitude and causes the rover to turn, thereby making crab-crawl mode infeasible, or
- If the substrate does not offer a sufficient level of traction for motion in crab-crawl resulting in 100% slip or the burying in the substrate.

2) Feasibility of Crab-crawl mode: If the propulsive force acting on the blades is negligible then the yawing torque is insignificantly low and the rover can move in crab-crawl mode. As discussed in Section II-A, the propulsive force magnitude drops drastically when the substrate fails under the stresses exerted by the helical drives. Thus, substrate failure is critical for crab-crawl motion. Whether the substrate fails depends on (1) the bulk properties of the substrate, and (2) normal and shear stresses acting on the substrate element located between two blades. The stresses acting on the substrate element depend on the wheel sinkage as the amount of sinkage determines the shape and size of the substrate element located between two blades. The sinkage in crab-crawl mode can be calculated using (4) and (5) as discussed in Section III-A.

3) Mode Selection Algorithm Steps: Based on the discussion in the above sections, the steps involved in mode selection are

Step 1: Assume the rover is moving in crab-crawl mode and determine the helical drive sinkage using Equations 4 and 5.
Step 2: Using the sinkage, calculate the dimensions of the substrate element located between two blades.
Step 3: Calculate the forces exerted by the drives on the substrate element (which are equal and opposite to the forces acting on the helical drives) using (1).
Step 4: Using the dimensions and forces acting on the substrate element, calculate the maximum shear stress and determine if the substrate fails, i.e., $\tau_{max} > \tau_{sub}$.
Step 5: If the substrate fails, choose *crab-crawl mode*. Otherwise, choose *screw mode*.
Thus, at the end of Step 5, a mode of locomotion is selected for a given substrate. Fig. 5 shows the mode selection algorithm and the steps discussed above

4) Energy Estimation and Path Planning: Once the mode of locomotion is selected, the required torque is calculated using either (2) for screw mode or (6) for crab-crawl mode. Consequently, for a constant angular speed, the power is estimated.

Path planning is formulated as a minimum energy optimization problem. Several candidate paths are created for going from the 'Start' point to the 'End' point. Each path spans over multiple terrains or substrates and the amount

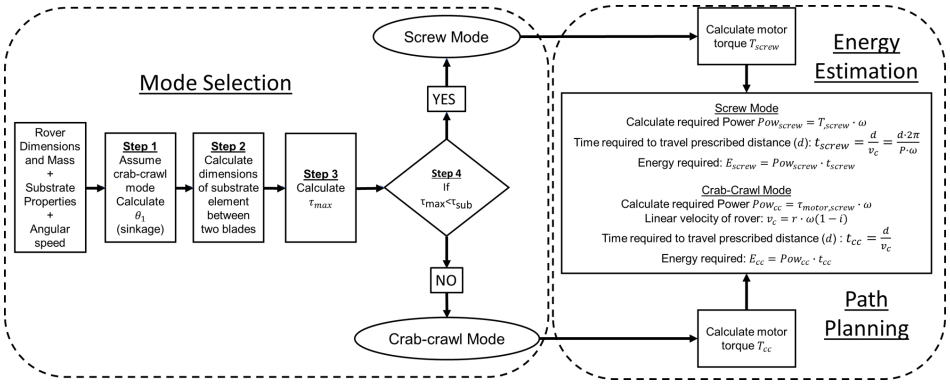

Fig. 5. Mode Selection, Energy Estimation, and Path Planning Algorithm Flowchart

TABLE I
BULK PROPERTIES OF SUBSTRATE

Property	Silty Sand	Clayey Soil	Compacted Snow
c	1.04	4.14	1.03
ϕ_{fric}	28	13	19.7
μ_k	0.2	0.35	0.16
k_c	0.99	13.19	4.37
k_{phi}	1528.43	692.15	196.72
n	1.1	0.5	1.6
K	1.5	2.76	1.8

of distance to be traveled on each substrate varies between paths. First, using the mode selection algorithm, either *screw* or *crab-crawl* mode is selected for each substrate. Then, for a fixed angular speed, the required torque and power are calculated. The time required to traverse each segment depends on the speed of the vehicle in the selected mode. For example, the rover moves $2\pi r/P$ time faster and takes a shorter amount of time to travel in crab-crawl mode with zero slip than it screw mode with $x_c = P \cdot n$ motion. Using the power calculated in the previous step and the amount of time it takes to traverse a segment, the required energy is calculated for each segment. Then, the total energy required to traverse the entire path is calculated by summing the energy required for each segment in the path. Finally, the path with the least amount of energy is chosen. Fig. 5 shows the energy calculation steps following the mode selection steps.

V. RESULTS

In this section, the algorithm is used for mode selection and path planning in the case of the rover traversing across a hypothetical landscape consisting of silty sand, clayey soil, and compact snow. The design of the landscape and distribution of terrains are shown in Fig. 6. The cylinder radius (r_c = 0.03175 m), blade height (h_b = 0.0133 m), length (l_{HD} = 0.3175 m), Pitch length (P = 0.0366 m) of the helical drive and the rover mass (m_{rover} = 40.0 kg) are kept constant throughout the analysis. The relevant bulk properties of the substrates are listed in Table I.

TABLE II
ENERGY ESTIMATION

	Distance (m)	Slip	Speed (m/s)	Energy (kJ)
Silty Sand	50	0.0	0.0997	0.913
Clayey Soil	40	N/A	0.0183	5.986
Snow	55	N/A	0.0183	4.116

A. Mode Selection

Fig. 6 shows that the algorithm chooses crab-crawl mode for silty sand and screw mode for both clayey soil and compacted snow. This is because the silty sand substrate fails under the stresses exerted by the rover, however, clayey soil, and compacted snow do not fail. The motor torque and power required to move in the different substrates have also been shown in Fig. 6, for a constant angular speed of $\omega = \pi rad/s$. The results show that the torque required to move in crab-crawl mode is lower than that required to move in screw mode.

B. Energy Estimation and Path Planning

The energy spent, distance covered, and rover speed in each substrate for the path in Fig. 6 are shown in Table II. As expected the rover's speed is higher in crab-crawl mode compared to screw mode. Three candidate paths - *A*, *B*, and *C*, are considered for path planning as shown in Fig. 7. Based on the results shown in Table III, Path *C* requires the least amount of energy although the rover travels the maximum distance going from the 'Start' to the 'End' point. Maximizing the amount of distance traveled in crab-crawl mode while minimizing the distance traveled in screw mode helps achieve the most optimal path.

VI. CONCLUSIONS

In this work, an algorithm for mode selection, energy estimation, and path planning for a multi-mode, helical drives-based vehicle was presented. The algorithm chose between screw and crab-crawl mode based on substrate bulk properties which determine whether the substrate fails under the stresses exerted by the drives. Additionally, the algorithm chose the lowest energy path out of several candidate paths

TABLE III
PATH PLANNING RESULTS

	Silty Sand		Clayey Soil		Compacted Snow			
Path	Distance (m)	Energy (kJ)	Distance (m)	Energy (kJ)	Distance (m)	Energy (kJ)	Total Distance (m)	Total Energy (kJ)
A	30	0.55	35	5.23	55	4.11	120	9.90
B	40	0.73	25	3.74	45	3.36	110	7.84
C	60	1.09	15	2.24	50	3.74	**125**	**7.08**

that the rover could take while traversing multiple types of terrains. Future work will focus on taking into consideration the effects of obstacle avoidance, turning maneuvers, and yawing maneuvers to switch between modes.

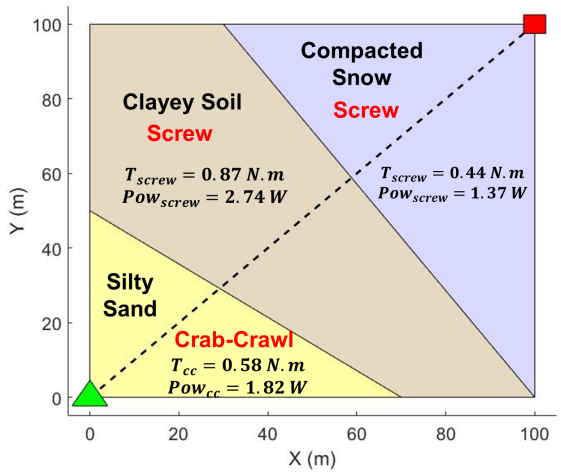

Fig. 6. A prescribed path across the landscape and the mode of locomotion used in each substrate. The green triangle represents the starting location and the red square represents the final location of the rover

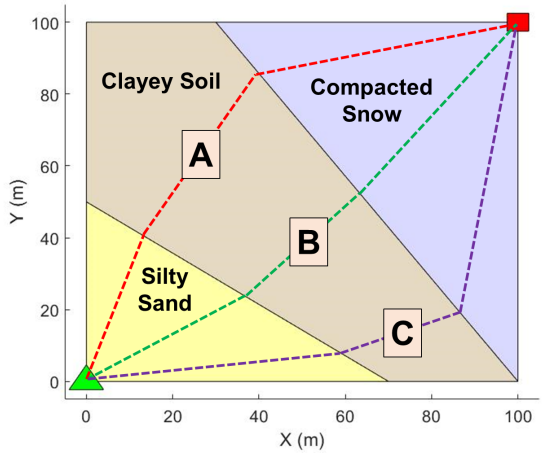

Fig. 7. Three candidate paths that the rover can traverse to get from starting location to the final location

REFERENCES

[1] L. Pedersen, M. Wagner, D. Apostolopoulos, and W. Whittaker, "Autonomous robotic meteorite identification in antarctica," in *Proceedings 2001 ICRA. IEEE International Conference on Robotics and Automation (Cat. No. 01CH37164)*, vol. 4. IEEE, 2001, pp. 4158–4165.

[2] L. Ray, A. Price, A. Streeter, D. Denton, and J. H. Lever, "The design of a mobile robot for instrument network deployment in antarctica," in *Proceedings of the 2005 IEEE International Conference on Robotics and Automation*. IEEE, 2005, pp. 2111–2116.

[3] C. Kunz, C. Murphy, H. Singh, C. Pontbriand, R. A. Sohn, S. Singh, T. Sato, C. Roman, K.-i. Nakamura, M. Jakuba, *et al.*, "Toward extraplanetary under-ice exploration: Robotic steps in the arctic," *Journal of Field Robotics*, vol. 26, no. 4, pp. 411–429, 2009.

[4] S. Beknalkar, M. Bryant, S. Darbha, and A. Mazzoleni, "Underwater dynamics, controls and trajectory tracking of an amphibious screw-propelled vehicle for arctic exploration," In Press.

[5] S. Beknalkar, A. Varanwal, R. Lynch, M. Bryant, and A. Mazzoleni, "Modeling and analysis of terrestrial locomotion dynamics of helical drive-propelled multi-terrain vehicles," in *ASME International Mechanical Engineering Congress and Exposition*, vol. 87639. American Society of Mechanical Engineers, 2023, p. V006T07A004.

[6] B. Donohue, S. Beknalkar, R. Bishop, M. Bryant, and A. Mazzoleni, "Modeling underwater propulsion of a helical drive using computational fluid dynamics for an amphibious rover," in *ASME International Mechanical Engineering Congress and Exposition*, vol. 87639. American Society of Mechanical Engineers, 2023, p. V006T07A045.

[7] B. Donohue, S. Beknalkar, M. Bryant, and A. Mazzoleni, "A dynamic model for underwater propulsion of an amphibious rover developed from kane's method," in *ASME International Mechanical Engineering Congress and Exposition*, vol. 87639. American Society of Mechanical Engineers, 2023, p. V006T07A012.

[8] A. Vadlamannati, S. Beknalkar, D. Best, M. Bryant, and A. Mazzoleni, "Design, prototyping, and experiments using small-scale helical drive rover for multi-terrain exploration," in *ASME International Mechanical Engineering Congress and Exposition*, vol. 87639. American Society of Mechanical Engineers, 2023, p. V006T07A078.

[9] R. Lynch, S. Beknalkar, R. Bishop, A. Crow, B. Donohue, C. Pacheco-Cay, A. Smith, A. Mazzoleni, and M. Bryant, "Design and construction of a terrestrial testing rig for experimentation and analysis of multi-terrain screw-propelled vehicle dynamics and performance."

[10] N. A. Olmedo, M. G. Lipsett, J. Yuen, and C. Milne, "Towards autonomous tailings and pit lake monitoring with amphibious robots," 2022.

[11] M. Green, T. McBryan, D. Mick, D. Nelson, and H. Marvi, "Regolith excavation performance of a screw-propelled vehicle," *Advanced Intelligent Systems*, vol. 5, no. 3, p. 2100125, 2023.

[12] K. Nagaoka and T. Kubota, "Modeling and analysis on exploration rover with screw drive mechanism over loose soil," in *Proceedings of the 10th International Symposium on Artificial Intelligence, Robotics and Automation in Space*, 2010, pp. 162–169.

[13] A. Thoesen, S. Ramirez, and H. Marvi, "Screw-powered propulsion in granular media: An experimental and computational study," in *2018 IEEE international conference on robotics and automation (ICRA)*. IEEE, 2018, pp. 4283–4288.

[14] J. Villacrés, M. Barczyk, and M. Lipsett, "Literature review on archimedean screw propulsion for off-road vehicles," *Journal of Terramechanics*, vol. 108, pp. 47–57, 2023.

[15] J.-Y. Wong and A. Reece, "Prediction of rigid wheel performance based on the analysis of soil-wheel stresses part i. performance of driven rigid wheels," *Journal of Terramechanics*, vol. 4, no. 1, pp. 81–98, 1967.